

Odd-even differences in the stability “peninsula” in the $106 \leq Z \leq 112$ region with the deformed relativistic Hartree-Bogoliubov theory in continuum

Xiao-Tao He^{✉*} and Jia-Wei Wu^{✉†}*College of Materials Science and Technology, Nanjing University of Aeronautics and Astronautics, Nanjing 210016, China*Kai-Yuan Zhang^{✉‡}*Institute of Nuclear Physics and Chemistry, China Academy of Engineering Physics, Mianyang, Sichuan 621900, China*Cai-Wan Shen[§]*School of Science, Huzhou University, Huzhou 313000, China*

(Received 5 March 2024; accepted 16 May 2024; published 1 July 2024)

The predictive power of the deformed relativistic Hartree-Bogoliubov theory in continuum (DRHBc) with density functional PC-PK1 is demonstrated for superheavy region ($101 \leq Z \leq 120$) by comparing with available experimental and evaluated data from AME2020. The DRHBc theory predicts 93 bound nuclei beyond the drip line $N = 258$ in the region of $106 \leq Z \leq 112$, which form a stability peninsula. The odd-even differences between odd- N and even- N nuclei are remarkable in the peninsula; the one-neutron separation energy of an odd- N nucleus is smaller than those of its neighboring even- N nuclei due to the blocking effect, and as a result the number of bound odd- N nuclei is less than that of bound even- N nuclei. The deformation effect is indispensable for the re-entrant stability beyond the drip line by significantly affecting the structure of single-particle levels around the Fermi energy. The interplay between deformation and pairing influences the location of the first bound odd- N nucleus in the peninsula. By examining the deformation effect at different orders, it is found that quadrupole deformation β_2 contributes predominantly to the appearance of stability peninsula, and the effects of higher-order deformations β_4 and β_6 are non-negligible.

DOI: [10.1103/PhysRevC.110.014301](https://doi.org/10.1103/PhysRevC.110.014301)

I. INTRODUCTION

Exploration of the limit of the nuclear existence is a prior topic in nuclear physics [1–4]. Along or near the β -stability line, the stable nuclei form the valley of stability. Starting from the β -stability line, the nuclear binding energy increases by adding neutrons, until the neutron drip line, beyond which the binding energy is not enough to prevent the last neutron(s) from escaping the nucleus. Therefore, the neutron drip line depicts the boundary of the nuclear landscape on the neutron-rich side. However, it was predicted in Ref. [5] that beyond the neutron drip line the binding energy may increase again with the neutron number. This phenomenon of re-entrant stability against particle emission might lead to a novel *peninsula* comprised of bound nuclei adjacent to the nuclear landscape [5].

To date, the existence of more than 3300 nuclides has been confirmed experimentally [6,7], and the masses of about 2500 among them have been measured [8–10]. The proton-rich boundary of the nuclear territory has been determined up to

neptunium ($Z = 93$) [11], but the neutron drip line is known only up to neon ($Z = 10$) [12]. The experimental exploration of very neutron-rich nuclei is extremely challenging, as most of them will remain beyond experimental capabilities in the foreseeable future. Thus, for heavier elements, the quest for the neutron drip line relies on theoretical models with predictive power.

During the past two decades, the phenomenon of re-entrant stability beyond the neutron drip line has been predicted in several studies. Skyrme Hartree-Fock-Bogoliubov calculations in the transformed harmonic oscillator (THO) basis have predicted the regions of re-entrant stability around $Z = 60$, 70, and 100, which was explained as due to the effects of neutron shell closures [3,5]. Similar phenomena have also been predicted and attributed to the local changes in the shell structure induced by deformation with relativistic Hartree-Bogoliubov (RHB) calculations in the harmonic oscillator (HO) basis [13]. Compared with the HO basis that is incapable of describing near-drip-line nuclei [14–17], the THO basis provides an improved asymptotic behavior [18,19]. However, both of them are less suitable than the coordinate-space solution for the description of nuclei with very diffuse density distributions [16,20]. The re-entrant stability has also been studied with the Skyrme Hartree-Fock plus Bardeen-Cooper-Schrieffer (BCS) theory [21–23], but the BCS theory cannot properly describe the pairing correlations in exotic nuclei

*Contact author: hext@nuaa.edu.cn†Contact author: wjw1998@nuaa.edu.cn‡Contact author: zhangky@caep.cn§Contact author: cwshen@zjhu.edu.cn

[24,25]. Instead, the Bogoliubov transformation provides a well-established method to treat pairing correlations in both stable and exotic nuclei in a unified way [26].

The covariant density functional theory (CDFT) has successfully described a variety of nuclear phenomena [24,25,27–31]. Based on the CDFT, by properly considering the effects of pairing and continuum, the relativistic continuum Hartree-Bogoliubov (RCHB) theory was developed with assumed spherical symmetry [15,32]. It has successfully described and predicted many phenomena [32–39], including the continuum effect on the limit of nuclear landscape [4].

Since most nuclei, except those around doubly magic nuclei, are deformed in the ground state, the RCHB theory is further developed to the deformed relativistic Hartree-Bogoliubov theory in continuum (DRHBc) by considering the effects of deformation, pairing, and continuum simultaneously [40,41]. The advantages of the DRHBc theory have been highlighted by many applications, e.g., to deformed halo nuclei [42–49]. With this theory, the nuclear mass table for even- Z nuclei has been constructed [50,51], and the peninsula of stability beyond the two-neutron drip line has been predicted [52–54]. In particular, the predictive power of the DRHBc theory combined with density functional PC-PK1 [55] for the masses of superheavy nuclei has been demonstrated [52].

In previous studies [52–54], the phenomenon of re-entrant stability based on the DRHBc theory has been discussed for only even-even nuclei. It is unclear whether there are bound odd nuclei in the stability peninsula. To answer this question, the masses and neutron separation energies of odd- A and odd-odd nuclei near the peninsula should be explored. In the description of odd nuclei, the blocking effect of the unpaired nucleon(s) that plays an important role in ground-state properties [56–59] needs to be considered. Accordingly, the DRHBc theory has been extended to incorporate the blocking effect based on both meson-exchange [60] and point-coupling [61] density functionals.

In this work, we first examine the predictive ability of the DRHBc theory for even-even, odd- A , and odd-odd nuclei in the superheavy region of $101 \leq Z \leq 120$. We then investigate the stability peninsula for isotopic chains from Sg ($Z = 106$) to Cn ($Z = 112$), with focus on exploring the possible existence of bound odd nuclei and the difference of their properties from those of even- N nuclei. This paper is organized as follows. In Sec. II, a brief theoretical framework is given. Numerical details and the blocking procedure are introduced in Sec. III. Results are presented and discussed in Sec. IV. Finally, a summary is made in Sec. V.

II. THEORETICAL FRAMEWORK

The details of the DRHBc theory can be found in Refs. [41,61,62]. Here, we briefly present its formalism. The RHB equation reads [63]

$$\begin{pmatrix} h_D - \lambda_\tau & \Delta \\ -\Delta^* & -h_D^* + \lambda_\tau \end{pmatrix} \begin{pmatrix} U_k \\ V_k \end{pmatrix} = E_k \begin{pmatrix} U_k \\ V_k \end{pmatrix}, \quad (1)$$

where λ_τ is the Fermi energy for neutrons or protons ($\tau = n$ or p), and E_k and $(U_k, V_k)^T$ are the quasiparticle energy and

wave function, respectively. h_D is the Dirac Hamiltonian,

$$h_D(\mathbf{r}) = \alpha \cdot \mathbf{p} + V(\mathbf{r}) + \beta[M + S(\mathbf{r})], \quad (2)$$

where $S(\mathbf{r})$ and $V(\mathbf{r})$ are the scalar and vector potentials, respectively. Δ is the pairing potential

$$\Delta(\mathbf{r}_1, \mathbf{r}_2) = V^{\text{PP}}(\mathbf{r}_1, \mathbf{r}_2)\kappa(\mathbf{r}_1, \mathbf{r}_2) \quad (3)$$

with the pairing tensor κ [56] and a density-dependent pairing force of zero range,

$$V^{\text{PP}}(\mathbf{r}_1, \mathbf{r}_2) = V_0 \frac{1}{2} (1 - P^\sigma) \delta(\mathbf{r}_1 - \mathbf{r}_2) \left(1 - \frac{\rho(\mathbf{r}_1)}{\rho_{\text{sat}}} \right), \quad (4)$$

in which V_0 is the pairing strength, ρ_{sat} denotes the saturation density of nuclear matter, and $\frac{1}{2}(1 - P^\sigma)$ represents the projector for the spin $S = 0$ component in the pairing channel. The pairing tensor, various densities, and potentials in coordinate space are expanded in terms of the Legendre polynomials,

$$f(\mathbf{r}) = \sum_{\lambda} f_{\lambda}(r) P_{\lambda}(\cos \theta), \quad \lambda = 0, 2, 4, \dots \quad (5)$$

To describe properly the possible large spatial extension of exotic nuclei, the RHB equations are solved in a Dirac Woods-Saxon basis [17,64], which has proven equivalent to coordinate-space solutions.

For an odd- A or odd-odd nucleus, the blocking effect of the unpaired nucleon(s) should be taken into account, which can be achieved in the RHB framework by the exchange of the quasiparticle wave functions $(V_{k_b}^*, U_{k_b}^*) \leftrightarrow (U_{k_b}, V_{k_b})$ and that of the energy $E_{k_b} \leftrightarrow -E_{k_b}$, in which k_b stands for the blocked state. More details for the treatment of odd systems in the DRHBc theory can be found in Refs. [60,61].

III. NUMERICAL DETAILS

Our calculations are carried out with the relativistic density functional PC-PK1 [55]. The pairing strength $V_0 = -325$ MeV fm³ and the saturation density $\rho_{\text{sat}} = 0.152$ fm⁻³ in Eq. (4), and a pairing window of 100 MeV is adopted. For the Dirac Woods-Saxon basis, an energy cutoff of $E_{\text{cut}}^+ = 300$ MeV and an angular momentum cutoff of $J_{\text{max}} = 23/2\hbar$ are adopted. In Eq. (5), the Legendre expansion is truncated at $\lambda_{\text{max}} = 10$ [65]. The above numerical details are the same as those used in the global mass table calculation over the nuclear chart [50,51].

In the present DRHBc theory, the blocking effect is included via the equal filling approximation [66], under which the time-odd components vanish and the time-reversal symmetry is conserved. Both the orbital-fixed blocking and the automatic blocking have been implemented in the DRHBc theory [61]. The former blocks separately the orbitals near the Fermi energy and takes the result with the lowest energy as the ground state [4]. However, the computational cost of this procedure can be extremely high for deformed superheavy nuclei. In the automatic blocking, the lowest quasiparticle orbital is always blocked during the iterative solution of the RHB equation, which can find in most cases the correct ground state with much less computational resources. Our calculations are

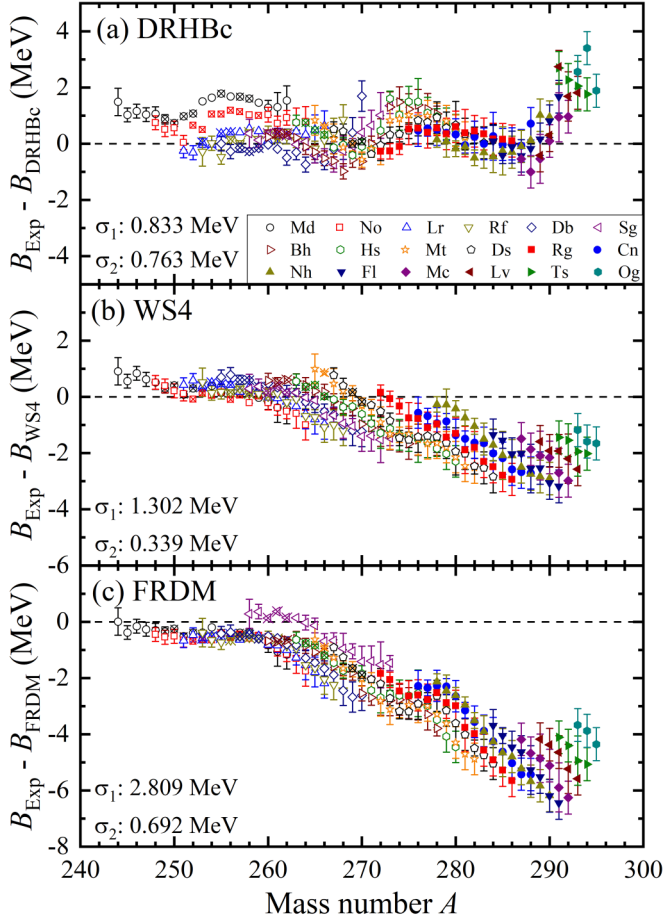


FIG. 1. Binding energy difference between the AME2020 data [8] and the results from (a) the DRHBc theory, (b) the WS4 mass model, and (c) the FRDM(2012) mass model for superheavy nuclei with $101 \leq Z \leq 118$. For $101 \leq Z \leq 110$, nuclei with experimental and evaluated data are shown by crossed and open symbols, respectively. For $111 \leq Z \leq 118$, nuclei with only evaluated data are shown by solid symbols. σ_1 is the rms deviation from a total of 240 available data, and σ_2 is that from 36 experimental ones.

performed first with the automatic blocking and then, if necessary, with the orbital-fixed one.

IV. RESULTS AND DISCUSSION

The predictive power of the DRHBc theory for the masses of even-even superheavy nuclei has been demonstrated [52] by comparing with the popular macroscopic-microscopic mass models WS4 [67] and FRDM (2012) [68]. In this work, we further examine the DRHBc description for superheavy odd- A and odd-odd nuclei. Figure 1(a) shows the difference in binding energy between DRHBc results and available data from AME2020 [8] for nuclei with $101 \leq Z \leq 118$, in comparison with those for WS4 in Fig. 1(b) and FRDM in Fig. 1(c). For 36 experimental data, the root-mean-square (rms) deviation σ_2 in the DRHBc calculation is 0.7663 MeV, on the same order of magnitude as 0.339 MeV by WS4 and 0.692 MeV by FRDM. However, after including 204 evaluated data, the rms deviation of the DRHBc results from the

total 240 data changes slightly to $\sigma_1 = 0.833$ MeV, in contrast to the remarkable increase to $\sigma_1 = 1.302$ MeV for WS4 and to $\sigma_1 = 2.809$ MeV for FRDM.

Table I shows the rms deviations of results based on the DRHBc theory, the WS4 mass model, and the FRDM mass model from the AME2020 data for all, even-even, odd- A , and odd-odd nuclei in the region of $101 \leq Z \leq 118$. It can be found that the description by the DRHBc theory is comparable to those by WS4 and FRDM for experimental data, and after including evaluated data the DRHBc description becomes superior. It is also noted that, compared to even-even nuclei, the rms deviation by the DRHBc theory becomes slightly larger for odd nuclei. This is because in the present DRHBc calculations, the time-odd components that might influence the rotational correction energy [69] are neglected. It would be relevant to explore the effect of time-odd components on binding energies and rotational correction energies for odd nuclei by using the recently developed time-odd DRHBc theory [70] in future works. Furthermore, a better alternative to include the rotational correction is the two-dimensional collective Hamiltonian (2DCH), which can estimate the beyond-mean-field dynamical correlation energies from rotations and vibrations for both well-deformed and near-spherical nuclei. The 2DCH has been implemented based on the DRHBc theory only for even-even nuclei [71,72], and its future extension to odd nuclei is desirable.

The reliable predictive power of the DRHBc theory for superheavy nuclei enables the exploration of novel phenomena far from the stability valley. In Refs. [52,54], a stability peninsula consisting of even-even bound nuclei beyond the neutron drip line has been predicted in the region of $106 \leq Z \leq 112$. It would be interesting to study whether odd- A and odd-odd nuclei exist in this peninsula. Figure 2 illustrates the one-neutron separation energy S_n for superheavy nuclei from Sg ($Z = 106$) to Cn ($Z = 112$) near the neutron drip line. The sudden decrease of S_n from positive to negative after $N = 258$ suggests it as a possible magic number. This is consistent with the previous prediction made by other CDFT studies [13,37,73]. In Refs. [52,54], the nucleus $^{370}\text{Sg}_{264}$ has a negative two-neutron separation energy, showing its instability against two-neutron emission. Here, it is stable against one-neutron emission with a positive one-neutron separation energy. The same situation also appears for other $N = 264$ isotones. For even- N nuclei in $107 \leq Z \leq 112$ isotopic chains, the stability beyond the drip line can be found in the regions of $280 \leq N \leq 286$, $276 \leq N \leq 288$, $272 \leq N \leq 290$, $270 \leq N \leq 290$, $268 \leq N \leq 292$, and $266 \leq N \leq 296$, respectively. However, the re-entrant stability for odd- N nuclei appears later and ends earlier than that for even- N nuclei. Specifically, there is no bound odd- N nucleus with $Z = 107$ and 108, and except for two nuclei $^{386}\text{Rg}_{275}$ and $^{389}\text{Cn}_{277}$ unstable against one-neutron emission, the odd- N nuclei in the regions of $277 \leq N \leq 283$, $275 \leq N \leq 283$, $269 \leq N \leq 291$, and $267 \leq N \leq 291$ are bound for $Z = 109, 110, 111$, and 112, respectively. The one-neutron separation energies of these bound odd- N nuclei are obviously smaller than those of their even- N neighbors, i.e., significant odd-even difference can be found in the one-neutron separation energy.

TABLE I. The rms deviations (in MeV) of results based on the DRHBc theory, the WS4 mass model, and the FRDM(2012) mass model from the AME2020 data for total, even-even, odd-A, and odd-odd nuclei in the region of $101 \leq Z \leq 118$. σ_1 and σ_2 represent the rms deviations from all available data and from only experimental data, respectively. The corresponding data numbers are given in parentheses.

	All		Even-even		Odd-A		Odd-odd	
	$\sigma_1(240)$	$\sigma_2(36)$	$\sigma_1(57)$	$\sigma_2(10)$	$\sigma_1(118)$	$\sigma_2(18)$	$\sigma_1(65)$	$\sigma_2(8)$
DRHBc	0.833	0.763	0.777	0.631	0.848	0.815	0.883	0.790
WS4	1.302	0.339	1.371	0.159	1.271	0.308	1.295	0.522
FRDM	2.809	0.692	2.796	0.864	2.774	0.648	2.881	0.526

We take Ds isotopes as examples to further study the odd-even difference in the one-neutron separation energy. Figure 3 shows the DRHBc calculated total energies of Ds isotopes near the drip line relative to that of $^{368}\text{Ds}_{258}$ and their deformation parameters β_2 . The results from calculations assuming spherical symmetry and neglecting pairing correlations are also shown for comparison. Here, the total energy equals negative binding energy, $E = -B$, namely, a lower total energy corresponds to a larger binding energy. By adding neutrons, the decrease (increase) of the total energy means the stability (instability) against neutron emission of the obtained nucleus. It can be found in Fig. 3(a) that the variation of the total energy versus N shows clear odd-even staggering in the DRHBc results. In particular, the total energy increases from an even- N nucleus to the next odd- N nucleus in regions of $258 \leq N \leq 273$ and $284 \leq N \leq 291$, indicating the instability against one-neutron emission of these odd- N nuclei. As a result, the number of bound odd- N nuclei in the stability peninsula ($275 \leq N \leq 283$) is 5, much less than that of bound even- N nuclei, 11.

In the DRHBc results shown in Fig. 3(b), the Ds isotopes with $N = 258, 260$, and 262 are spherical while those with $N = 259, 261$, and 263 exhibit slight oblate deformation with small negative β_2 due to the polarization effect. For $N \geq 264$, β_2 becomes larger than 0.05 and continues to increase with N , accompanied by the emergence of neutron emitters and bound nuclei. In the spherical results shown in Fig. 3(a), the total energy of ^{368}Ds is lower than those of heavier isotopes, which means that without deformation no bound nucleus exists beyond the neutron drip line. Therefore, the deformation effects, which make the nuclear system more stable by lowering its total energy, play an indispensable role in the appearance of the stability peninsula. Meanwhile, the spherical results exhibit more pronounced odd-even differences in the total energy compared with the deformed results.

In the results without pairing shown in Fig. 3(a), after $N = 263$, the total energy keeps decreasing gradually until $N = 291$. No visible odd-even difference is found in the total energy, and the numbers of bound odd- N and even- N nuclei only differ by 1. Therefore, the odd-even differences between odd- N and even- N nuclei stem from the effects of pairing correlations. Both deformation and pairing effects contribute to the sophisticated phenomenon of re-entrant stability with odd-even differences. It can also be found in Fig. 3(b) that without pairing most nuclei become more deformed, indicating that pairing correlations might reduce nuclear deformation, which is consistent with the DRHBc + PC-PK1 results for the halo nucleus ^{19}B [45].

To further examine the contribution of pairing, we show in Fig. 4 the neutron, proton, and total pairing energies of Ds isotopes near the drip line. While the proton pairing energy varies steadily with increasing N , there are obvious odd-even differences in the neutron pairing energy. Due to the blocking effects of the unpaired neutron, the neutron pairing energy of an odd- N nucleus is smaller than those of its even- N neighbors in absolute value. This results in odd-even differences in the total pairing energy, the total energy, the one-neutron separation energy, and finally the stability against neutron emission.

To investigate the microscopic mechanism behind the re-entrant stability, we illustrate the single-neutron orbitals around the Fermi energy for $^{368,369,383,384,385}\text{Ds}$ in Fig. 5. In Fig. 5(a), the gap between the highest occupied orbital and the lowest unoccupied orbital in the spherical nucleus ^{368}Ds is approximately 3 MeV, supporting a shell closure at $N = 258$. The valence neutrons in this nucleus occupy the bound orbital $4p_{1/2}$. With one neutron added, the nucleus ^{369}Ds becomes slightly deformed, and its valence neutron occupies an orbital split from $1k_{15/2}$ that is embedded in continuum, making it unstable against one-neutron emission. With more neutrons added, the heavier isotopes deviate more from spherical shape.

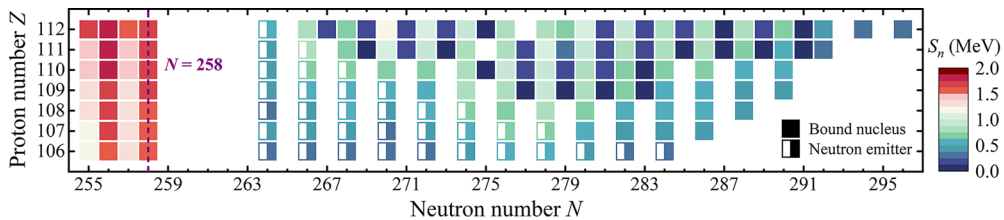


FIG. 2. One-neutron separation energies for nuclei with $106 \leq Z \leq 112$ near the neutron drip line as a function of the neutron number N and the proton number Z . The solid squares represent bound nuclei, and the semisolid squares represent nuclei that are bound against one-neutron emission but unbound against multineutron emission. The dashed line depicts the predicted magic number $N = 258$.

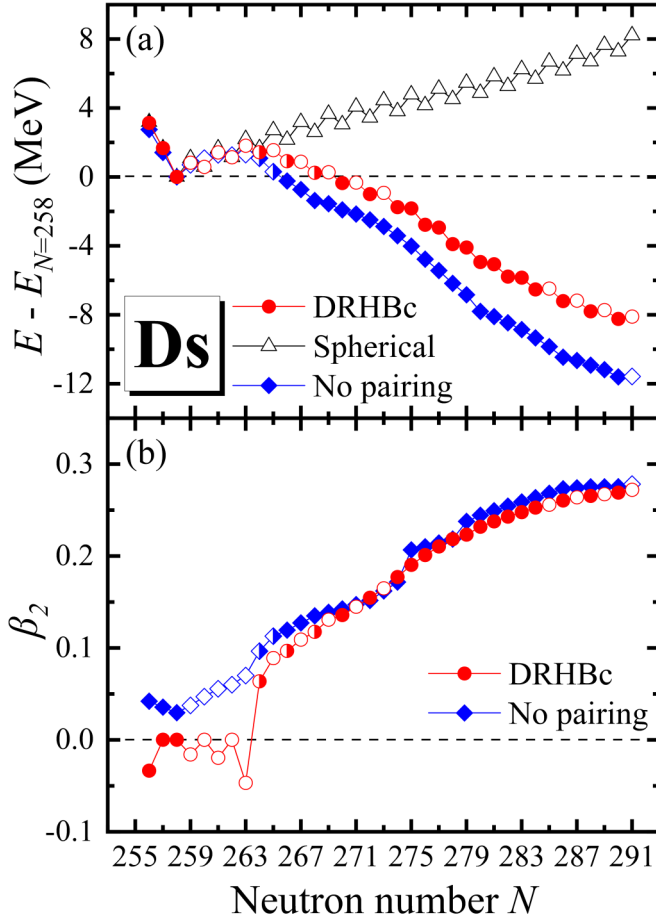


FIG. 3. The DRHBC calculated (a) total energies of Ds isotopes near the drip line relative to that of ^{368}Ds ($N = 258$) and (b) deformation parameters β_2 for these isotopes as functions of the neutron number N . The DRHBC results assuming spherical symmetry ($\lambda_{\text{max}} = 0$) and neglecting pairing correlations are also shown for comparison. The solid, open, and semisolid symbols represent nuclei that are bound, unbound, and bound against one-neutron emission but unbound against multineutron emission, respectively.

In Fig. 5(c), the nucleus ^{383}Ds is deformed with $\beta_2 = 0.165$, and several down-sloping orbitals cross the continuum threshold and become bound. Due to the loss of the pairing energy as shown in Fig. 4, the total energy of ^{383}Ds is higher than that of ^{382}Ds . In Fig. 5(d), with one more neutron added, the deformation parameter for ^{384}Ds increases to 0.177, and one more negative-parity orbital, $1/2^-$, becomes bound. The one-neutron, two-neutron, and multineutron separation energies of ^{384}Ds are all positive, making it a bound nucleus. In Fig. 5(e), the deformation parameter increases further to 0.190 for ^{385}Ds . Although the pairing energy is suppressed by the blocking effects, the extra total energy lowered by deformation makes ^{385}Ds stable against one-neutron emission. Therefore, while nuclear deformation plays an essential role in the re-entrant stability by significantly affecting the shell structure, the interplay between deformation and pairing influences the location of the first bound odd- N nucleus in the peninsula.

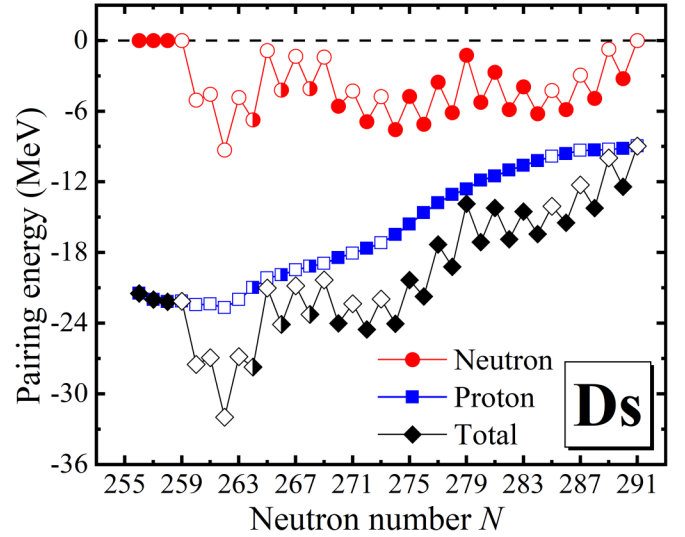


FIG. 4. The DRHBC calculated neutron, proton, and total pairing energies as functions of the neutron number N for Ds isotopes near the drip line. The solid, open, and semisolid symbols represent nuclei that are bound, unbound, and bound against one-neutron emission but unbound against multineutron emission, respectively.

It has been demonstrated that the effects of higher-order deformations are crucial for the ground-state properties of superheavy nuclei in a previous CDFT study [74]. To reveal the effects of deformation at different order, we show in Fig. 6 the calculated total energies of Ds isotopes near the drip line relative to that of ^{368}Ds with different Legendre expansion truncation in Eq. (5). Namely, $\lambda_{\text{max}} = 2$ corresponds to the calculation only including quadrupole deformation β_2 , $\lambda_{\text{max}} = 4$ corresponds to the calculation including quadrupole and hexadecapole deformations β_2 and β_4 , and so on. As already seen in Fig. 3, when assuming spherical symmetry, there is no bound nucleus beyond $N = 258$ but clear odd-even difference in the total energy. After including quadrupole deformation, the re-entrant stability appears, with 11 even- N and 4 odd- N bound nuclei. It can be also found that the odd-even differences in the total energy are reduced. After further including hexadecapole deformation, the odd-even staggering in the total energy appears further reduced, and the number of bound odd- N nuclei in the stability peninsula increases to 8. While the number of even- N nuclei keeps unchanged as 11 with increasing λ_{max} , that of bound odd- N nuclei decreases, respectively, to 6 and 5 in the results with $\lambda_{\text{max}} = 6$ and 10. Actually, the results with $\lambda_{\text{max}} = 6$ and 10 look quite close, indicating that the effects of β_8 and β_{10} are marginal for the stability peninsula. In other words, from a view of expansion, the results suggest that the calculations are essentially converged with λ_{max} .

Finally, we note that the DRHBC calculations also predict many neutron emitters in the peninsula of stability. The neutron radioactivity is one of the most appealing topics in modern nuclear physics [75], e.g., the two-neutron emitter ^{16}Be observed in 2012 [76] has been further investigated recently [77]. Another recent experiment that discovered new isotopes ^{160}Os and ^{156}W has revealed enhanced stability of the

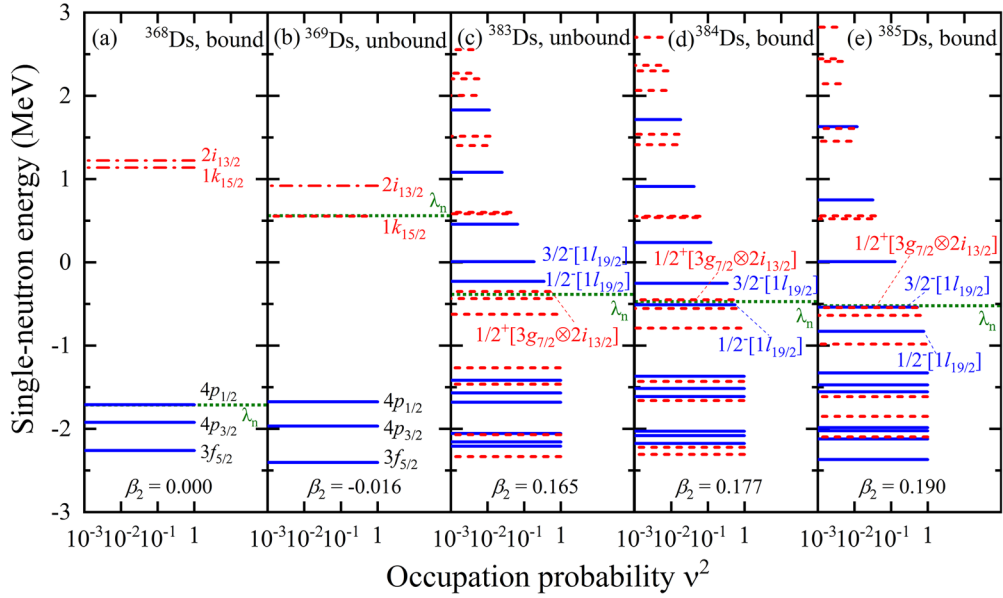


FIG. 5. Single-neutron orbitals in the canonical basis around the Fermi energy λ_n (dotted line) versus the occupation probability ν^2 for $^{368,369,383,384,385}\text{Ds}$ in the DRHbc calculations. For the spherical (near-spherical) nucleus ^{368}Ds (^{369}Ds), orbitals are labeled by quantum numbers nj , and the unoccupied orbitals are shown by dotted-dashed lines. For deformed nuclei $^{383,384,385}\text{Ds}$, orbitals around λ_n are labeled by quantum numbers Ω^π , and their major components are given in the square brackets.

$N = 82$ shell closure toward the proton drip line by analyzing α -decay energies and half-lives [78]. This finding implies that the unobserved ^{164}Pb , despite being beyond the proton drip line, could be a doubly magic nucleus with increased stability [78]. The half-life estimation can be achieved by the DRHbc + WKB approach, which has been successful in describing α -decay half-lives of even-even nuclei with $74 \leq Z \leq 92$ [79] and the one-proton emission half-life of ^{149}Lu [80] as well as predicting the multineutron emission half-lives of bound Ba and Sm isotopes beyond the neutron drip line [53]. Therefore, it is quite encouraging to estimate the half-lives of the DRHbc predicted neutron emitters in future works, which may provide

reference for experimental search of possible stability beyond the drip line.

V. SUMMARY

In summary, the predictive power of the DRHbc theory is demonstrated for the masses of superheavy nuclei with $101 \leq Z \leq 118$. For the 36 (240) measured (measured plus evaluated) mass data compiled in AME2020, the DRHbc description accuracy is 0.763 (0.833) MeV, in contrast to 0.339 (1.302) MeV by WS4 and 0.692 (2.809) MeV by FRDM. The DRHbc theory predicts 93 bound nuclei with $106 \leq Z \leq 112$

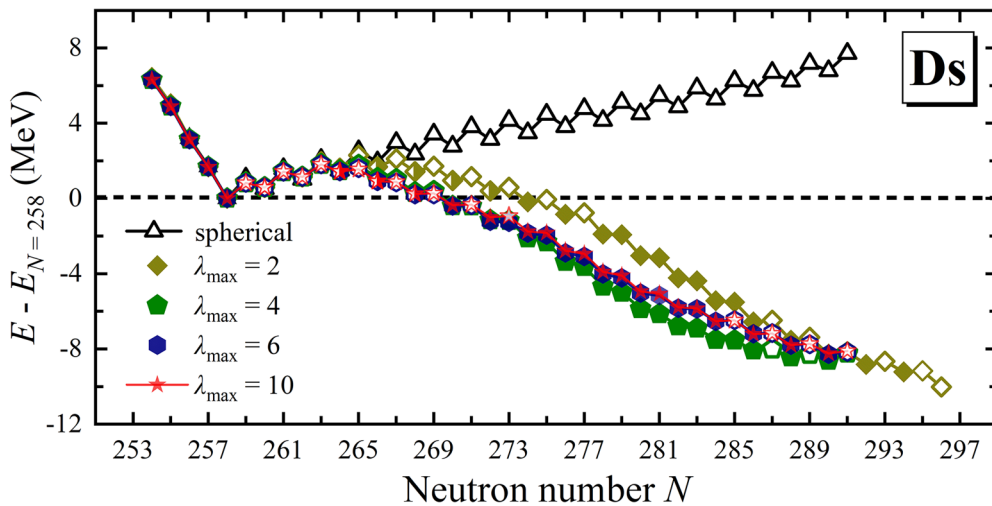


FIG. 6. The DRHbc calculated total energies of Ds isotopes near the drip line relative to that of ^{368}Ds as functions of the neutron number N with the Legendre expansion truncated at different orders. The solid, open, and semisolid symbols represent nuclei that are bound, unbound, and bound against one-neutron emission but unbound against multineutron emission, respectively.

beyond the primary neutron drip line $N = 258$, which form a stability peninsula adjacent to the nuclear landscape. Significant odd-even differences between odd- N and even- N nuclei are found in the peninsula; an odd- N nucleus is less stable than its neighboring even- N nuclei with a smaller one-neutron separation energy. As a result, the re-entrant stability for odd- N nuclei appears later and ends earlier than that for even- N nuclei along an isotopic chain.

The underlying mechanism behind the formation of stability peninsula and the odd-even difference are investigated in detail by taking Ds isotopes near the drip line as examples. There is no re-entrant stability when assuming spherical symmetry, demonstrating the indispensable role of deformation in the formation of stability peninsula. In the results without pairing, the total energy varies smoothly between odd- N and even- N nuclei, demonstrating that the odd-even differences stem from the pairing effects; specifically, the neutron pairing energy in an odd- N nucleus is suppressed by the blocking effects of the unpaired neutron.

By investigating the single-neutron orbitals around the Fermi energy for $^{368,369,383,384,385}\text{Ds}$, it is found that the deformation effect significantly affects the nuclear shell structure. With the increasing deformation, more and more down-sloping orbitals cross the continuum threshold and become bound. The even- N nucleus ^{380}Ds first becomes bound due to this deformation effect, while its neighboring odd- N nuclei are still unbound. With more neutrons added, the deformation

increases further, and the odd- N nucleus ^{380}Ds gains enough binding energy from the deformation effect to become stable against one-neutron emission. The interplay between deformation and pairing can influence the location of the first bound odd- N nucleus in the stability peninsula.

By examining the deformation effect at different orders, it is found that quadrupole deformation β_2 contributes predominantly to the re-entrant stability beyond the neutron drip line. Hexadecapole deformation β_4 weakens the odd-even differences and, thus, increases the number of odd- N nuclei in the peninsula. The results considering higher-order deformations up to β_6 and to β_{10} appear very close, indicating that the effects of β_8 and β_{10} are marginal for the stability peninsula, and the calculations are essentially converged with λ_{max} from a view of expansion.

ACKNOWLEDGMENTS

Helpful discussions with members of the DRHBc Mass Table Collaboration are gratefully acknowledged. This work is supported by the National Natural Science Foundation of China (Grants No. U2032138, No. 12075085, No. 12275082, and No. 12305125), the National Key R&D Program of China (Contract No. 2023YFA1606503), the Sichuan Science and Technology Program (Grant No. 2024NSFSC1356), and the High-performance Computing Platform of Huzhou University.

-
- [1] M. Thoennessen, Current status and future potential of nuclide discoveries, *Rep. Prog. Phys.* **76**, 056301 (2013).
- [2] M. Thoennessen, *The Discovery of Isotopes* (Springer, New York, 2016).
- [3] J. Erler, N. Birge, M. Kortelainen, W. Nazarewicz, E. Olsen, A. M. Perhac, and M. Stoitsov, The limits of the nuclear landscape, *Nature (London)* **486**, 509 (2012).
- [4] X. Xia, Y. Lim, P. Zhao, H. Liang, X. Qu, Y. Chen, H. Liu, L. Zhang, S. Zhang, Y. Kim, and J. Meng, The limits of the nuclear landscape explored by the relativistic continuum Hartree-Bogoliubov theory, *At. Data Nucl. Data Tables* **121–122**, 1 (2018).
- [5] M. V. Stoitsov, J. Dobaczewski, W. Nazarewicz, S. Pittel, and D. J. Dean, Systematic study of deformed nuclei at the drip lines and beyond, *Phys. Rev. C* **68**, 054312 (2003).
- [6] M. Thoennessen, 2022 update of the discoveries of nuclides, *Int. J. Mod. Phys. E* **32**, 2330001 (2023).
- [7] Discovery of Nuclides Project, <https://frib.msu.edu/public/nuclides>.
- [8] M. Wang, W. Huang, F. Kondev, G. Audi, and S. Naimi, The AME 2020 atomic mass evaluation (II). Tables, graphs and references, *Chin. Phys. C* **45**, 030003 (2021).
- [9] F. Kondev, M. Wang, W. Huang, S. Naimi, and G. Audi, The NUBASE2020 evaluation of nuclear physics properties, *Chin. Phys. C* **45**, 030001 (2021).
- [10] W. Huang, M. Wang, F. Kondev, G. Audi, and S. Naimi, The AME 2020 atomic mass evaluation (I). Evaluation of input data, and adjustment procedures, *Chin. Phys. C* **45**, 030002 (2021).
- [11] Z. Y. Zhang, Z. G. Gan, H. B. Yang, L. Ma, M. H. Huang, C. L. Yang, M. M. Zhang, Y. L. Tian, Y. S. Wang, M. D. Sun, H. Y. Lu, W. Q. Zhang, H. B. Zhou, X. Wang, C. G. Wu, L. M. Duan, W. X. Huang, Z. Liu, Z. Z. Ren, S. G. Zhou *et al.*, New isotope ^{220}Np : Probing the robustness of the $N = 126$ shell closure in neptunium, *Phys. Rev. Lett.* **122**, 192503 (2019).
- [12] D. S. Ahn, N. Fukuda, H. Geissel, N. Inabe, N. Iwasa, T. Kubo, K. Kusaka, D. J. Morrissey, D. Murai, T. Nakamura, M. Ohtake, H. Otsu, H. Sato, B. M. Sherrill, Y. Shimizu, H. Suzuki, H. Takeda, O. B. Tarasov, H. Ueno, Y. Yanagisawa *et al.*, Location of the neutron dripline at fluorine and neon, *Phys. Rev. Lett.* **123**, 212501 (2019).
- [13] A. V. Afanasjev, S. E. Agbemava, D. Ray, and P. Ring, Nuclear landscape in covariant density functional theory, *Phys. Lett. B* **726**, 680 (2013).
- [14] J. Dobaczewski, W. Nazarewicz, T. R. Werner, J. F. Berger, C. R. Chinn, and J. Dechargé, Mean-field description of ground-state properties of drip-line nuclei: Pairing and continuum effects, *Phys. Rev. C* **53**, 2809 (1996).
- [15] J. Meng, Relativistic continuum Hartree-Bogoliubov theory with both zero range and finite range Gogny force and their application, *Nucl. Phys. A* **635**, 3 (1998).
- [16] S.-G. Zhou, J. Meng, S. Yamaji, and S.-C. Yang, Deformed relativistic Hartree theory in coordinate space and in harmonic oscillator basis, *Chin. Phys. Lett.* **17**, 717 (2000).
- [17] S. G. Zhou, J. Meng, and P. Ring, Spherical relativistic Hartree theory in a Woods-Saxon basis, *Phys. Rev. C* **68**, 034323 (2003).

- [18] M. Stoitsov, P. Ring, D. Vretenar, and G. A. Lalazissis, Solution of relativistic Hartree-Bogoliubov equations in configurational representation: Spherical neutron halo nuclei, *Phys. Rev. C* **58**, 2086 (1998).
- [19] M. V. Stoitsov, W. Nazarewicz, and S. Pittel, New discrete basis for nuclear structure studies, *Phys. Rev. C* **58**, 2092 (1998).
- [20] Y. N. Zhang, J. C. Pei, and F. R. Xu, Hartree-Fock-Bogoliubov descriptions of deformed weakly bound nuclei in large coordinate spaces, *Phys. Rev. C* **88**, 054305 (2013).
- [21] K. A. Gridnev, D. K. Gridnev, V. G. Kartavenko, V. E. Mitroshin, V. N. Tarasov, D. V. Tarasov, and W. Greiner, On stability of the neutron rich oxygen isotopes, *Int. J. Mod. Phys. E* **15**, 673 (2006).
- [22] W. Greiner and V. Zagrebaev, Extension of the periodic system: Superheavy, superneutronic, superstrange, antimatter nuclei, *Nucl. Phys. A* **834**, 323c (2010).
- [23] V. N. Tarasov, K. A. Gridnev, D. K. Gridnev, D. V. Tarasov, and W. Greiner, Stability peninsulas on the neutron drip line, *Int. J. Mod. Phys. E* **22**, 1350009 (2013).
- [24] J. Meng, H. Toki, S. Zhou, S. Zhang, W. Long, and L. Geng, Relativistic continuum Hartree Bogoliubov theory for ground-state properties of exotic nuclei, *Prog. Part. Nucl. Phys.* **57**, 470 (2006).
- [25] J. Meng and S. G. Zhou, Halos in medium-heavy and heavy nuclei with covariant density functional theory in continuum, *J. Phys. G* **42**, 093101 (2015).
- [26] J. Dobaczewski, H. Flocard, and J. Treiner, Hartree-Fock-Bogolyubov description of nuclei near the neutron-drip line, *Nucl. Phys. A* **422**, 103 (1984).
- [27] P. Ring, Relativistic mean field theory in finite nuclei, *Prog. Part. Nucl. Phys.* **37**, 193 (1996).
- [28] D. Vretenar, A. Afanasjev, G. Lalazissis, and P. Ring, Relativistic Hartree-Bogoliubov theory: Static and dynamic aspects of exotic nuclear structure, *Phys. Rep.* **409**, 101 (2005).
- [29] T. Nikšić, D. Vretenar, and P. Ring, Relativistic nuclear energy density functionals: Mean-field and beyond, *Prog. Part. Nucl. Phys.* **66**, 519 (2011).
- [30] J. Meng, J. Peng, S. Q. Zhang, and P. W. Zhao, Progress on tilted axis cranking covariant density functional theory for nuclear magnetic and antimagnetic rotation, *Front. Phys.* **8**, 55 (2013).
- [31] S.-G. Zhou, Multidimensionally constrained covariant density functional theories—Nuclear shapes and potential energy surfaces, *Phys. Scr.* **91**, 063008 (2016).
- [32] J. Meng and P. Ring, Relativistic Hartree-Bogoliubov description of the neutron halo in ^{11}Li , *Phys. Rev. Lett.* **77**, 3963 (1996).
- [33] J. Meng and P. Ring, Giant halo at the neutron drip line, *Phys. Rev. Lett.* **80**, 460 (1998).
- [34] S. Q. Zhang, J. Meng, S. G. Zhou, and J. Y. Zeng, Giant neutron halo in exotic calcium nuclei, *Chin. Phys. Lett.* **19**, 312 (2002).
- [35] J. Meng, K. Sugawara-Tanabe, S. Yamaji, P. Ring, and A. Arima, Pseudospin symmetry in relativistic mean field theory, *Phys. Rev. C* **58**, R628 (1998).
- [36] J. Meng, K. Sugawara-Tanabe, S. Yamaji, and A. Arima, Pseudospin symmetry in Zr and Sn isotopes from the proton drip line to the neutron drip line, *Phys. Rev. C* **59**, 154 (1999).
- [37] W. Zhang, J. Meng, S. Zhang, L. Geng, and H. Toki, Magic numbers for superheavy nuclei in relativistic continuum Hartree-Bogoliubov theory, *Nucl. Phys. A* **753**, 106 (2005).
- [38] Y. Kuang, X. L. Tu, J. T. Zhang, K. Y. Zhang, and Z. P. Li, Systematic study of elastic proton-nucleus scattering using relativistic impulse approximation based on covariant density functional theory, *Eur. Phys. J. A* **59**, 160 (2023).
- [39] X. H. Wu, C. Pan, K. Y. Zhang, and J. Hu, Nuclear mass predictions of the relativistic continuum Hartree-Bogoliubov theory with the kernel ridge regression, *Phys. Rev. C* **109**, 024310 (2024).
- [40] S.-G. Zhou, J. Meng, P. Ring, and E.-G. Zhao, Neutron halo in deformed nuclei, *Phys. Rev. C* **82**, 011301(R) (2010).
- [41] L. Li, J. Meng, P. Ring, E.-G. Zhao, and S.-G. Zhou, Deformed relativistic Hartree-Bogoliubov theory in continuum, *Phys. Rev. C* **85**, 024312 (2012).
- [42] X.-X. Sun, J. Zhao, and S.-G. Zhou, Shrunk halo and quenched shell gap at $N = 16$ in ^{22}C : Inversion of sd states and deformation effects, *Phys. Lett. B* **785**, 530 (2018).
- [43] K. Y. Zhang, D. Y. Wang, and S. Q. Zhang, Effects of pairing, continuum, and deformation on particles in the classically forbidden regions for Mg isotopes, *Phys. Rev. C* **100**, 034312 (2019).
- [44] Z. H. Yang, Y. Kubota, A. Corsi, K. Yoshida, X.-X. Sun, J. G. Li, M. Kimura, N. Michel, K. Ogata, C. X. Yuan, Q. Yuan, G. Authalet, H. Baba, C. Caesar, D. Calvet, A. Delbart, M. Dozono, J. Feng, F. Flavigny, J.-M. Gheller *et al.*, Quasifree neutron knockout reaction reveals a small s -orbital component in the Borromean nucleus ^{17}B , *Phys. Rev. Lett.* **126**, 082501 (2021).
- [45] X.-X. Sun, Deformed two-neutron halo in ^{19}B , *Phys. Rev. C* **103**, 054315 (2021).
- [46] K. Y. Zhang, P. Papakonstantinou, M.-H. Mun, Y. Kim, H. Yan, and X.-X. Sun, Collapse of the $N = 28$ shell closure in the newly discovered ^{39}Na nucleus and the development of deformed halos towards the neutron dripline, *Phys. Rev. C* **107**, L041303 (2023).
- [47] K. Y. Zhang, S. Q. Yang, J. L. An, S. S. Zhang, P. Papakonstantinou, M.-H. Mun, Y. Kim, and H. Yan, Missed prediction of the neutron halo in ^{37}Mg , *Phys. Lett. B* **844**, 138112 (2023).
- [48] K. Y. Zhang, S. Q. Zhang, and J. Meng, Possible neutron halo in the triaxial nucleus ^{42}Al , *Phys. Rev. C* **108**, L041301 (2023).
- [49] J.-L. An, K.-Y. Zhang, Q. Lu, S.-Y. Zhong, and S.-S. Zhang, A unified description of the halo nucleus ^{37}Mg from microscopic structure to reaction observables, *Phys. Lett. B* **849**, 138422 (2024).
- [50] K. Zhang, M.-K. Cheoun, Y.-B. Choi, P. S. Chong, J. Dong, Z. Dong, X. Du, L. Geng, E. Ha, X.-T. He, C. Heo, M. C. Ho, E. J. In, S. Kim, Y. Kim, C.-H. Lee, J. Lee, H. Li, Z. Li, T. Luo *et al.* (DRHBc Mass Table Collaboration), Nuclear mass table in deformed relativistic Hartree-Bogoliubov theory in continuum, I: Even-even nuclei, *At. Data Nucl. Data Tables* **144**, 101488 (2022).
- [51] P. Guo, X. Cao, K. Chen, Z. Chen, M.-K. Cheoun, Y.-B. Choi, P. C. Lam, W. Deng, J. Dong, P. Du, X. Du, K. Duan, X. Fan, W. Gao, L. Geng, E. Ha, X.-T. He, J. Hu, J. Huang, K. Huang *et al.* (DRHBc Mass Table Collaboration), Nuclear mass table in deformed relativistic Hartree-Bogoliubov theory in continuum, II: Even-Z nuclei, *At. Data Nucl. Data Tables* **158**, 101661 (2024).
- [52] K. Y. Zhang, X. T. He, J. Meng, C. Pan, C. W. Shen, C. Wang, and S. Q. Zhang, Predictive power for superheavy nuclear mass and possible stability beyond the neutron drip line in deformed relativistic Hartree-Bogoliubov theory in continuum, *Phys. Rev. C* **104**, L021301 (2021).

- [53] C. Pan, K. Y. Zhang, P. S. Chong, C. Heo, M. C. Ho, J. Lee, Z. P. Li, W. Sun, C. K. Tam, S. H. Wong, R. W.-Y. Yeung, T. C. Yiu, and S. Q. Zhang, Possible bound nuclei beyond the two-neutron drip line in the $50 \leq Z \leq 70$ region, *Phys. Rev. C* **104**, 024331 (2021).
- [54] X. T. He, W. Chen, K. Y. Zhang, and C. W. Shen, Possible existence of bound nuclei beyond neutron drip lines driven by deformation, *Chin. Phys. C* **45**, 101001 (2021).
- [55] P. W. Zhao, Z. P. Li, J. M. Yao, and J. Meng, New parametrization for the nuclear covariant energy density functional with a point-coupling interaction, *Phys. Rev. C* **82**, 054319 (2010).
- [56] P. Ring and P. Schuck, *The Nuclear Many-Body Problem* (Springer Science & Business Media, New York, 2004).
- [57] X.-X. Sun, J. Zhao, and S.-G. Zhou, Study of ground state properties of carbon isotopes with deformed relativistic Hartree-Bogoliubov theory in continuum, *Nucl. Phys. A* **1003**, 122011 (2020).
- [58] H. Nakada and K. Takayama, Intertwined effects of pairing and deformation on neutron halos in magnesium isotopes, *Phys. Rev. C* **98**, 011301(R) (2018).
- [59] H. Kasuya and K. Yoshida, Hartree-Fock-Bogoliubov theory for odd-mass nuclei with a time-odd constraint and application to deformed halo nuclei, *Prog. Theor. Exp. Phys.* **2021**, 013D01 (2021).
- [60] L. Li, J. Meng, P. Ring, E.-G. Zhao, and S.-G. Zhou, Odd systems in deformed relativistic Hartree-Bogoliubov theory in continuum, *Chin. Phys. Lett.* **29**, 042101 (2012).
- [61] C. Pan, M.-K. Cheoun, Y.-B. Choi, J. Dong, X. Du, X.-H. Fan, W. Gao, L. Geng, E. Ha, X.-T. He, J. Huang, K. Huang, S. Kim, Y. Kim, C.-H. Lee, J. Lee, Z. Li, Z.-R. Liu, Y. Ma, J. Meng *et al.* (DRHBc Mass Table Collaboration), Deformed relativistic Hartree-Bogoliubov theory in continuum with a point-coupling functional. II. Examples of odd Nd isotopes, *Phys. Rev. C* **106**, 014316 (2022).
- [62] K. Zhang, M.-K. Cheoun, Y.-B. Choi, P. S. Chong, J. Dong, L. Geng, E. Ha, X. He, C. Heo, M. C. Ho, E. J. In, S. Kim, Y. Kim, C.-H. Lee, J. Lee, Z. Li, T. Luo, J. Meng, M.-H. Mun, Z. Niu *et al.* (DRHBc Mass Table Collaboration), Deformed relativistic Hartree-Bogoliubov theory in continuum with a point-coupling functional: Examples of even-even Nd isotopes, *Phys. Rev. C* **102**, 024314 (2020).
- [63] H. Kucharek and P. Ring, Relativistic field theory of superfluidity in nuclei, *Z. Phys. A* **339**, 23 (1991).
- [64] K. Y. Zhang, C. Pan, and S. Q. Zhang, Optimized Dirac Woods-Saxon basis for covariant density functional theory, *Phys. Rev. C* **106**, 024302 (2022).
- [65] C. Pan, K. Zhang, and S. Zhang, Multipole expansion of densities in the deformed relativistic Hartree-Bogoliubov theory in continuum, *Int. J. Mod. Phys. E* **28**, 1950082 (2019).
- [66] S. Perez-Martin and L. M. Robledo, Microscopic justification of the equal filling approximation, *Phys. Rev. C* **78**, 014304 (2008).
- [67] N. Wang, M. Liu, X. Wu, and J. Meng, Surface diffuseness correction in global mass formula, *Phys. Lett. B* **734**, 215 (2014).
- [68] P. Möller, A. Sierk, T. Ichikawa, and H. Sagawa, Nuclear ground-state masses and deformations: FRDM(2012), *At. Data Nucl. Data Tables* **109–110**, 1 (2016).
- [69] P. W. Zhao, L. S. Song, B. Sun, H. Geissel, and J. Meng, Crucial test for covariant density functional theory with new and accurate mass measurements from Sn to Pa, *Phys. Rev. C* **86**, 064324 (2012).
- [70] C. Pan, K. Zhang, and S. Zhang, Nuclear magnetism in the deformed halo nucleus ^{31}Ne , *Phys. Lett. B* **855**, 138792 (2024).
- [71] W. Sun, K.-Y. Zhang, C. Pan, X.-H. Fan, S. Zhang, and Z.-P. Li, Beyond-mean-field dynamical correlations for nuclear mass table in deformed relativistic Hartree-Bogoliubov theory in continuum, *Chin. Phys. C* **46**, 064103 (2022).
- [72] X. Y. Zhang, Z. M. Niu, W. Sun, and X. W. Xia, Nuclear charge radii and shape evolution of Kr and Sr isotopes with the deformed relativistic Hartree-Bogoliubov theory in continuum, *Phys. Rev. C* **108**, 024310 (2023).
- [73] J. J. Li, W. H. Long, J. Margueron, and N. Van Giai, Superheavy magic structures in the relativistic Hartree-Fock-Bogoliubov approach, *Phys. Lett. B* **732**, 169 (2014).
- [74] X.-Q. Wang, X.-X. Sun, and S.-G. Zhou, Microscopic study of higher-order deformation effects on the ground states of superheavy nuclei around ^{270}Hs , *Chin. Phys. C* **46**, 024107 (2022).
- [75] M. Pfützner, M. Karny, L. V. Grigorenko, and K. Riisager, Radioactive decays at limits of nuclear stability, *Rev. Mod. Phys.* **84**, 567 (2012).
- [76] A. Spyrou, Z. Kohley, T. Baumann, D. Bazin, B. A. Brown, G. Christian, P. A. DeYoung, J. E. Finck, N. Frank, E. Lunderberg, S. Mosby, W. A. Peters, A. Schiller, J. K. Smith, J. Snyder, M. J. Strongman, M. Thoennessen, and A. Volya, First observation of ground state dineutron decay: ^{16}Be , *Phys. Rev. Lett.* **108**, 102501 (2012).
- [77] B. Monteagudo, F. M. Marqués, J. Gibelin, N. A. Orr, A. Corsi, Y. Kubota, J. Casal, J. Gómez-Camacho, G. Authélet, H. Baba, C. Caesar, D. Calvet, A. Delbart, M. Dozono, J. Feng, F. Flavigny, J.-M. Gheller, A. Giganon, A. Gillibert, K. Hasegawa *et al.*, Mass, spectroscopy, and two-neutron decay of ^{16}Be , *Phys. Rev. Lett.* **132**, 082501 (2024).
- [78] H. B. Yang, Z. G. Gan, Y. J. Li, M. L. Liu, S. Y. Xu, C. Liu, M. M. Zhang, Z. Y. Zhang, M. H. Huang, C. X. Yuan, S. Y. Wang, L. Ma, J. G. Wang, X. C. Han, A. Rohilla, S. Q. Zuo, X. Xiao, X. B. Zhang, L. Zhu, Z. F. Yue *et al.*, Discovery of new isotopes ^{160}Os and ^{156}W : Revealing enhanced stability of the $N = 82$ shell closure on the neutron-deficient side, *Phys. Rev. Lett.* **132**, 072502 (2024).
- [79] Y.-B. Choi, C.-H. Lee, M.-H. Mun, S. Choi, and Y. Kim, α -decay half-lives for even-even isotopes of W to U, *Phys. Rev. C* **109**, 054310 (2024).
- [80] Y. Xiao, S.-Z. Xu, R.-Y. Zheng, X.-X. Sun, L.-S. Geng, and S.-S. Zhang, One-proton emission from $^{148-151}\text{Lu}$ in the DRHBc+WKB approach, *Phys. Lett. B* **845**, 138160 (2023).